

- [1] Sun, X., Meng, F., Liu, J., McKechnie, J., & Yang, J. (2019). Life cycle energy use and greenhouse gas emission of lightweight vehicle – A body-in-white design. *Journal of Cleaner Production*, 220, 1–8.
- [2] Sato, F. E. K., & Nakata, T. (2021). Analysis of the impact of vehicle lightweighting on recycling benefits considering life cycle energy reductions. *Resources, Conservation and Recycling*, 164(June 2020), 105118.
- [3] Kawajiri, K., Kobayashi, M., & Sakamoto, K. (2020). Lightweight materials equal lightweight greenhouse gas emissions?: A historical analysis of greenhouse gases of vehicle material substitution. *Journal of Cleaner Production*, 253, 119805.
- [4] He, X., Kim, H. C., Wallington, T. J., Zhang, S., Shen, W., De Kleine, R., Keoleian, G. A., Ma, R., Zheng, Y., Zhou, B., & Wu, Y. (2020). Cradle-to-gate greenhouse gas (GHG) burdens for aluminum and steel production and cradle-to-grave GHG benefits of vehicle lightweighting in China. *Resources, Conservation and Recycling*, 152(May 2019)..
- [5] Arowosola, A., & Gaustad, G. (2019). Estimating increasing diversity and dissipative loss of critical metals in the aluminum automotive sector. *Resources, Conservation and Recycling*, 150(May), 104382.
- [6] Ferreira, V., Egizabal, P., Popov, V., García de Cortázar, M., Irazustabarrena, A., López-Sabirón, A. M., & Ferreira, G. (2019). Lightweight automotive components based on nanodiamond-reinforced aluminium alloy: A technical and environmental evaluation. *Diamond and Related Materials*, 92(December 2018), 174–186.
- [7] Han, L., Thornton, M., & Shergold, M. (2010). A comparison of the mechanical behaviour of self-piercing riveted and resistance spot welded aluminium sheets for the automotive industry. *Materials and Design*, 31(3), 1457–1467.
- [8] Lertora, E. (2013). Comparison of AA 2024 T3 friction stir welded and riveted overlap joints with the addition of a pressurization test. *Materials and Design*, 49, 259–266.
- [9] Honaryar, A., Iranmanesh, M., Liu, P., & Honaryar, A. (2020). Numerical and experimental investigations of outside corner joints welding deformation of an aluminum autonomous catamaran vehicle by inherent strain/deformation FE analysis. *Ocean Engineering*, 200(February), 106976.
- [10] Seloane, W. T., Mpofu, K., Ramatsetse, B. I., & Modungwa, D. (2020). Conceptual design of intelligent reconfigurable welding fixture for rail car manufacturing industry. *Procedia CIRP*, 91, 583–593.
- [11] Shen, L., Chen, H., Che, X., & Wang, Y. (2020). Stress corrosion cracking behavior of laser-MIG hybrid welded 7B05-T5 aluminum alloy. *Corrosion*

Science, 165(August 2019), 108417.

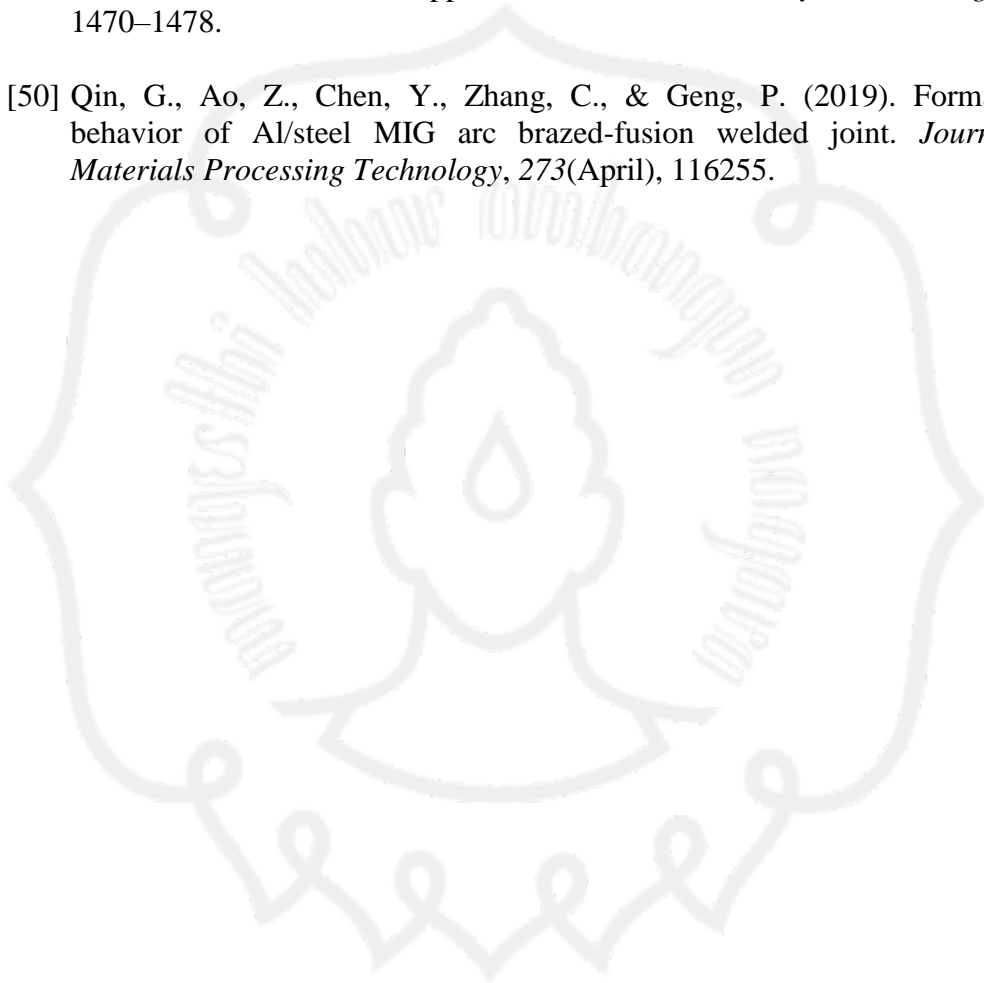
- [12] Ahn, J., Chen, L., He, E., Dear, J. P., & Davies, C. M. (2018). Optimisation of process parameters and weld shape of high power Yb-fibre laser welded 2024-T3 aluminium alloy. *Journal of Manufacturing Processes*, 34(May), 70–85.
- [13] Gou, G., Zhang, M., Chen, H., Chen, J., Li, P., & Yang, Y. P. (2015). Effect of humidity on porosity, microstructure, and fatigue strength of A7N01S-T5 aluminum alloy welded joints in high-speed trains. *Materials and Design*, 85, 309–317.
- [14] Xie, B., Li, Y., Li, S., Hu, S., Jin, H., & Zhou, F. (2020). Performance of composite polyester filter with magnetic NdFeB particles on filtering welding fume particles. *Powder Technology*, 368, 245–252.
- [15] Sivabalan, S., Sridhar, R., Parthiban, A., & Sathiskumar, G. (2020). Experimental investigations of mechanical behavior of friction stir welding on aluminium alloy 6063. *Materials Today: Proceedings*, xxxx.
- [16] Varshney, D., & Kumar, K. (2020). Application and use of different aluminium alloys with respect to workability, strength and welding parameter optimization. *Ain Shams Engineering Journal*, xxxx.
- [17] Mercan, E., Ayan, Y., & Kahraman, N. (2020). Investigation on joint properties of AA5754 and AA6013 dissimilar aluminum alloys welded using automatic GMAW. *Engineering Science and Technology, an International Journal*, 23(4), 723–731.
- [18] Yang, X., Chen, H., Zhu, Z., Cai, C., & Zhang, C. (2019). Effect of shielding gas flow on welding process of laser-arc hybrid welding and MIG welding. *Journal of Manufacturing Processes*, 38(February), 530–542.
- [19] Bitharas, I., McPherson, N. A., McGhie, W., Roy, D., & Moore, A. J. (2018). Visualisation and optimisation of shielding gas coverage during gas metal arc welding. *Journal of Materials Processing Technology*, 255(December 2017), 451–462.
- [20] Naidu, D. S., Ozcelik, S., & Moore, K. L. (2003). Chapter 2 - Gas Metal Arc Welding: Modeling. *Modeling, Sensing and Control of Gas Metal Arc Welding*, 9–93.
- [21] Zhao, S., Lou, Y., Chiu, A. P. Y., & He, D. (2018). Modelling the skip-and-resurgence of Japanese encephalitis epidemics in Hong Kong. *Journal of Theoretical Biology*, 454, 1–10.
- [22] Wahab, M. A. (2014). *Manual Metal Arc Welding and Gas Metal Arc Welding*. In *Comprehensive Materials Processing* (Vol. 6). Elsevier.
- [23] Ashidh, K., Santha Kumari, A., Sumesh, A., & Rajasekaran, N. (2015). Influence of Stick-Slip Effect on Gas Metal Arc Welding. *Applied*

Mechanics and Materials, 813–814, 438–445.

- [24] A. Silva-Magalhães, J. De Backer, J. Martin, and G. Bolmsjö, “In-situ temperature measurement in friction stir welding of thick section aluminium alloys,” *J. Manuf. Process.*, vol. 39, no. February, pp. 12–17, 2019.
- [25] Starke, E. A., & Rashed, H. M. M. A. (2017). Alloys: Aluminum. Reference Module in Materials Science and Materials Engineering.
- [26] Vargel, C. (2020). Aluminium alloy series. *Corrosion of Aluminium*, 17–20.
- [27] Singh, H., Raina, A., & Irfan Ul Haq, M. (2018). Effect of TiB₂ on mechanical and tribological properties of aluminium alloys - A review. *Materials Today: Proceedings*, 5(9), 17982–17988.
- [28] Mattson, S. (2012). Welding of aluminium. *Welding Processes Handbook*, 207–220.
- [29] American Welding Society. (2014). *Structural Welding Code Aluminium*. American Standart National Institute, 6-2013.
- [30] Hull, M. J., & Abraham, J. L. (2002). Aluminum welding fume-induced pneumoconiosis. *Human Pathology*, 33(8), 819–825.
- [31] Hedberg, Y. S., Wei, Z., McCarrick, S., Romanovski, V., Theodore, J., Westin, E. M., Wagner, R., Persson, K. A., Karlsson, H. L., & Odnevall Wallinder, I. (2021). Welding fume nanoparticles from solid and flux-cored wires: Solubility, toxicity, and role of fluorides. *Journal of Hazardous Materials*, 413(September 2020), 125273.
- [32] Simanjuntak, R., Muhayat, N., Prabowo, A. R., Saputro, Y. C. N., & Triyono. (2020). Effect of environment on the defects of welded aluminum AA 1100. *AIP Conference Proceedings*, 2217(April).
- [33] Zhou, G., Zhang, L., Liu, R., Sun, B., Kong, Y., & Huang, Z. (2021). Numerical simulation investigation for the pollution characteristics of dust particles in the fully mechanized mining face under different air humidity conditions. *Journal of Environmental Chemical Engineering*, 9(6), 106861.
- [34] Wang, H. Q., Huang, C. H., Liu, D., Zhao, F. Y., Sun, H. B., Wang, F. F., Li, C., Kou, G. X., & Ye, M. Q. (2012). Fume transports in a high rise industrial welding hall with displacement ventilation system and individual ventilation units. *Building and Environment*, 52, 119–128.
- [35] Vishnyakov, V. I., Kiro, S. A., Oprya, M. V., & Ennan, A. A. (2017). Effects of shielding gas temperature and flow rate on the welding fume particle size distribution. *Journal of Aerosol Science*, 114(September), 55–61.

- [36] Permenaker. (2018). Peraturan Menteri Tenaga Kerja No 5/2018 K3 Lingkungan Kerja. *Peraturan Menteri Ketenagakerjaan Republik Indonesia No 5 Tahun 2018*, 5, 1–258. <https://jdih.kemnaker.go.id/keselamatan-kerja.html>
- [37] Han, Y., Xue, S., Fu, R., & Zhang, P. (2019). Effect of hydrogen content in ER5183 welding wire on the tensile strength and fracture morphology of Al–Mg MIG weld. *Vacuum*, 166(March), 218–225.
- [38] Bai, Y., Gao, H. M., Wu, L., Ma, Z. H., & Cao, N. (2010). Influence of plasma-MIG welding parameters on aluminum weld porosity by orthogonal test. *Transactions of Nonferrous Metals Society of China (English Edition)*, 20(8), 1392–1396.
- [39] Junus, S. (2011). Pengaruh Besar Aliran Gas terhadap Cacat Porositas dan Struktur Mikro Hasil Pengelasan MIG pada Paduan Aluminium 5083. *Jurnal ROTOR*, Vol. 4(No. 1), 22–31.
- [40] Davis, J. R. (1993). *ASM Handbook Aluminum and Aluminum Alloys*.
- [41] Cetine, H., & Ayvaz, M. (2014). Microstructure and mechanical properties of aa 5083 and aa 6061 welds joined with aisi5 and aisi12wires. *Materialpruefung/Materials Testing*, 56(10), 884–890.
- [42] Syahroni, N., Winando, S. S., & Mulyadi, Y. (2021). *Influence Analysis of Shielding Gas Flow Rate and Purity Level Variation on GMAW Welding Process to Microstructure of Alumunium 5083*. 5(1), 18–22.
- [43] Zhan, X., Zhao, Y., Liu, Z., Gao, Q., & Bu, H. (2018). Microstructure and porosity characteristics of 5A06 aluminum alloy joints using laser-MIG hybrid welding. *Journal of Manufacturing Processes*, 35(September), 437–445.
- [44] Shahsavari, P., & Rezaei Ashtiani, H. R. (2020). Effects of Preheating and Cooling Rate on the Microstructure and Mechanical Properties of Tungsten Inert Gas Welded Joints of AA5083-H321 Aluminum Alloy. *Journal of Materials Engineering and Performance*, 29(10), 6790–6801.
- [45] Chen, R. Y., Chu, H. Y., Lai, C. C., & Wu, C. T. (2015). Effects of annealing temperature on the mechanical properties and sensitization of 5083-H116 aluminum alloy. *Proceedings of the Institution of Mechanical Engineers, Part L: Journal of Materials: Design and Applications*, 229(4), 339–346.
- [46] Han, X., Yang, Z., Ma, Y., Shi, C., & Xin, Z. (2020). Porosity distribution and mechanical response of laser-MIG hybrid butt welded 6082-T6 aluminum alloy joint. *Optics and Laser Technology*, 132(May), 106511.

- [47] Zhang, Q., Wang, T., Yao, Z., & Zhu, M. (2018). Materialia Modeling of hydrogen porosity formation during solidification of dendrites and irregular eutectics in Al – Si alloys. *Materialia*, 4(July), 211–220.
- [48] Kumarsingh, S., Mohan Tiwari, R., Kumar, A., Kumar, S., Qasimmurtaza, & Kumar, S. (2018). Mechanical Properties and Micrstructure of Al-5083 by TIG. *Materials Today: Proceedings*, 5(1), 819–822.
- [49] Jebaraj, A. V., Aditya, K. V. V., Kumar, T. S., Ajaykumar, L., & Deepak, C. R. (2019). Mechanical and corrosion behaviour of aluminum alloy 5083 and its weldment for marine applications. *Materials Today: Proceedings*, 22, 1470–1478.
- [50] Qin, G., Ao, Z., Chen, Y., Zhang, C., & Geng, P. (2019). Formability behavior of Al/steel MIG arc brazed-fusion welded joint. *Journal of Materials Processing Technology*, 273(April), 116255.





LAMPIRAN

Lampiran 1. Pengujian Kualitas Udara Ruang Pengelasan

Tabel Hasil Pengukuran Welding Fume

Waktu (s)	Variasi								
	H1 V1	H1 V2	H1 V3	H2 V1	H2 V2	H2 V3	H3 V1	H3 V2	H3 V3
0	48	51	54	33	30	172	1223	944	496
10	171	275	379	191	230	451	1060	781	643
20	957	1032	1097	825	929	1331	1630	1206	1156
30	1337	1278	1209	1269	1393	1515	1803	1456	1415
40	1418	1421	1414	1467	1533	1597	1774	1501	1528
50	1258	1409	1550	1519	1568	1591	1740	1506	1598
60	1272	1418	1554	1510	1514	1528	1578	1403	1557
70	1316	1379	1432	1464	1556	1578	1526	1477	1544
80	1361	1331	1291	1474	1577	1548	1587	1562	1524
90	1445	1575	1695	1533	1557	1549	1704	1702	1560
100	1494	1668	1832	1596	1644	1476	1845	1807	1638
110	1524	1576	1618	1701	1697	1513	1875	1801	1683
120	1564	1526	1478	1740	1717	1544	1931	1830	1731
130	1488	924	900	1717	1669	1533	2000	1904	1699
140	1159	573	527	1575	1579	1465	2000	1956	1571
150	915	299	223	1249	1346	1153	2000	1933	1322
160	797	221	185	939	1088	907	1823	1600	1134
170	689	186	205	795	851	781	1555	1449	980
180	599	163	230	674	736	689	1347	1336	878
190	550	137	234	581	589	618	1175	1232	758
200	489	120	231	476	474	558	1037	1167	632
210	464	118	231	374	382	525	934	1080	540
220	399	110	201	307	301	485	868	1019	464
230	308	105	195	269	260	451	799	957	406
240	273	95	189	222	231	440	740	915	366
250	254	91	185	211	213	421	679	868	338
260	235	84	176	206	199	406	645	835	313
270	225	80	170	206	179	391	610	788	281
280	209	70	150	200	161	373	558	795	268
290	192	66	152	195	152	344	504	779	259
300	189	71	146	196	150	333	447	779	250
310	185	73	135	194	147	330	402	783	253
320	182	68	128	183	146	330	356	783	232
330	177	66	119	168	136	308	331	770	230
340	166	61	109	161	135	302	320	756	220
350	153	54	105	152	130	297	325	756	213

Lampiran 2. Hasil Pengujian Kekerasan

Tabel Hasil Uji Kekerasan Mikro Vickers

Variasi Jarak	H1V1					H1V2					H1V3				
	1	2	3	Rata-Rata	Deviasi	1	2	3	Rata-Rata	Deviasi	1	2	3	Rata-Rata	Deviasi
0	95	96.1	95.5	95.53	0.550757	93	95.3	93.2	93.83333	1.274101	92	92.4	93	92.46667	0.503322
0.5	96.4	96	96.2	96.20	0.2	93.9	94.9	93.5	94.1	0.72111	94	93.2	92.1	93.1	0.953939
1	96.9	96.1	95.1	96.03	0.90185	95	95.1	94.5	94.86667	0.321455	95.8	95	93.4	94.73333	1.22202
1.5	96	97	95	96.00	1	94.6	95.4	95.6	95.2	0.52915	96.8	94.5	93.2	94.83333	1.823001
2	97	95.4	96	96.13	0.80829	95	95.4	96	95.46667	0.503322	96.2	94.4	95	95.2	0.916515
2.5	93.5	94.1	93.4	93.67	0.378594	93	92.1	93.7	92.93333	0.802081	92.4	93.4	93.6	93.13333	0.64291
3	97	96.8	96.4	96.73	0.305505	94	95	96	95	1	96	96.5	96.6	96.36667	0.321455
3.5	97.2	98	98	97.73	0.46188	97	97.1	97.8	97.3	0.43589	97	96.5	96.1	96.53333	0.450925
4	97.8	97.1	96.7	97.20	0.556776	95	96	98	96.33333	1.527525	98	97.8	96.1	97.3	1.044031
4.5	98.2	97.7	97.1	97.67	0.550757	95.6	95.1	97.7	96.13333	1.379613	98.7	95.2	96.2	96.7	1.802776
5	98	97.5	97	97.50	0.5	96.7	96	95.6	96.1	0.556776	97.5	96.4	97.4	97.1	0.608276
5.5	97.6	97.9	98	97.83	0.208167	96.7	96.2	96	96.3	0.360555	97.5	96.7	97.6	97.26667	0.493288
6	98.1	98	97.5	97.87	0.321455	96.8	96.2	96.1	96.36667	0.378594	97.3	97.1	97.3	97.23333	0.11547
6.5	98	97.8	98	97.93	0.11547	96	97.1	96	96.36667	0.635085	98.2	95.3	98	97.16667	1.619671
7	99	97	97.1	97.70	1.126943	96.9	96.5	96.7	96.7	0.2	98.3	95.7	98.2	97.4	1.473092

Variasi	H2V1					H2V2					H2V3				
	1	2	3	Rata-Rata	Deviasi	1	2	3	Rata-Rata	Deviasi	1	2	3	Rata-Rata	Deviasi
Jarak															
0	96.4	93.6	93.6	94.53333	1.616581	92.6	92.3	91	91.96667	0.85049	88.5	87.2	87.5	87.73333	0.680686
0.5	95.1	94.1	94.3	94.5	0.52915	93	93.4	92.3	92.9	0.556776	89	89.3	88	88.76667	0.680686
1	95.3	95	93.8	94.7	0.793725	93.2	93.1	91	92.43333	1.24231	92.2	91.2	89.4	90.93333	1.41892
1.5	95.8	93.7	94.6	94.7	1.053565	91.6	91.4	91.3	91.43333	0.152753	89.9	87.3	89.2	88.8	1.345362
2	96.4	95.1	94.2	95.23333	1.106044	92	91.2	92.5	91.9	0.655744	90	87.1	88.3	88.46667	1.457166
2.5	93	92.4	93.1	92.83333	0.378594	89	89.7	90.3	89.66667	0.650641	88	87.2	87.4	87.53333	0.416333
3	97	95	96.1	96.03333	1.001665	95	93.5	93.9	94.13333	0.776745	93.5	93.1	92.6	93.06667	0.450925
3.5	97	96.3	96.4	96.56667	0.378594	96	93.3	95.6	94.96667	1.457166	93	93.4	92.6	93	0.4
4	97.3	97.8	96.6	97.23333	0.602771	94.1	94.4	93.3	93.93333	0.568624	93.1	93.8	93.1	93.33333	0.404145
4.5	98	97.2	97.3	97.5	0.43589	94	93.7	92	93.23333	1.078579	93.2	94	93.5	93.56667	0.404145
5	98.1	97	96.5	97.2	0.818535	96.1	94.2	95.3	95.2	0.953939	94	95.1	94.1	94.4	0.608276
5.5	97	96.2	97.1	96.76667	0.493288	95.9	93.7	94.2	94.6	1.153256	93.3	93.8	96.1	94.4	1.493318
6	99.5	98.1	98.6	98.73333	0.70946	96	96.3	96.8	96.36667	0.404145	95.5	94.7	95.7	95.3	0.52915
6.5	99.8	98.4	97.1	98.43333	1.350309	96.9	97	96.3	96.73333	0.378594	96.3	95.2	97.1	96.2	0.953939
7	100	98.1	98.4	98.83333	1.021437	96.2	95.1	96.3	95.86667	0.665833	95.6	95.4	93.3	94.76667	1.274101

Variasi	H3V1					H3V2					H3V3				
	1	2	3	Rata-Rata	Deviasi	1	2	3	Rata-Rata	Deviasi	1	2	3	Rata-Rata	Deviasi
Jarak															
0	90	91.4	90.4	90.6	0.72111	88	90.1	87.4	88.5	1.417745	90.2	85.2	89.4	88.26667	2.685765
0.5	91.5	91.2	90.3	91	0.6245	86.1	87.6	89.1	87.6	1.5	89	88.3	84.3	87.2	2.535744
1	91.6	92.8	88.1	90.83333	2.441994	87	88.7	88.4	88.03333	0.907377	90.9	87.3	86.3	88.16667	2.419366
1.5	89.7	88.9	90.1	89.56667	0.61101	87.1	87.9	88.1	87.7	0.52915	90	83.1	86.3	86.46667	3.453018
2	91.2	91	90.8	91	0.2	87.2	88.6	88.2	88	0.72111	88.3	87.4	85.6	87.1	1.374773
2.5	88	86.1	88.5	87.53333	1.266228	86	88.3	89.2	87.83333	1.650253	88	87.1	85.2	86.76667	1.429452
3	92	92.5	93.1	92.53333	0.550757	89	91.2	91.2	90.46667	1.270171	91	91.9	87.3	90.06667	2.437895
3.5	92.6	92.1	92.1	92.26667	0.288675	89.4	90.2	90.6	90.06667	0.61101	91.3	89.9	88	89.73333	1.656301
4	92.7	92.5	93.8	93	0.7	89.9	90.1	90.2	90.06667	0.152753	91.6	91.3	88.3	90.4	1.824829
4.5	93.4	92.8	92.3	92.83333	0.550757	88.5	89.7	92.4	90.2	1.997498	92	92.4	90.3	91.56667	1.115049
5	92.7	91.7	92.8	92.4	0.608276	89.5	90.5	90.1	90.03333	0.503322	92.4	93.4	88.7	91.5	2.475884
5.5	93.2	91.1	89.7	91.33333	1.761628	91	91.2	90.3	90.83333	0.472582	92	92.4	89.3	91.23333	1.686219
6	94	93.2	94.1	93.76667	0.493288	92.1	91.3	92.6	92	0.655744	92.7	92.3	89.4	91.46667	1.800926
6.5	94.5	94.2	93.2	93.96667	0.680686	92	93.5	92.3	92.6	0.793725	92.6	93.8	90.2	92.2	1.83303
7	94	93	92	93	1	93	93.2	93.1	93.1	0.1	93.5	91.2	89.7	91.46667	1.913984

Lampiran 3. Hasil Pengujian Uji Tarik

Tabel Hasil Pengujian Tarik

Variasi	Specimen	t (mm)	w(mm)	l (mm)	A (mm ²)	Fm (N)	UTS (MPa)	Rata-rata (MPa)	Standar deviasi	Δl	Elongasi	Rata rata	Standar deviasi	
H1V1	1	6	12.5	200	75	21830	291.0667	290.5	6.28945024	15.3	8%	7%	0.00742181	4250.584
	2	6	12.1	200	72.6	20610	283.8843			12.4	6%			
	3	6	12.1	200	72.6	21520	296.4187			13.3	7%			
H1V2	1	6	12.1	200	72.6	19940	274.6556	274.5	2.20214254	8.9	4%	4%	0.00028868	6192.407
	2	6	12.2	200	73.2	19930	272.2678			8.9	4%			
	3	6	12	200	72	19920	276.6667			8.8	4%			
H1V3	1	6	12.7	200	76.2	20450	268.3727	272.7	4.43767588	9.1	5%	4%	0.00292973	6292.373
	2	6	12.3	200	73.8	20460	277.2358			8.9	4%			
	3	6	12.5	200	75	20430	272.4			8	4%			
H2V1	1	6	12.6	200	75.6	20670	273.4127	275.1	1.85003277	10.2	5%	6%	0.00550757	4797.761
	2	6	12.6	200	75.6	20770	274.7354			12.2	6%			
	3	6	12.5	200	75	20780	277.0667			12	6%			
H2V2	1	6	12.8	200	76.8	20670	269.1406	273.4	3.99785496	9.3	5%	5%	0.00259808	5695.993
	2	6	12.5	200	75	20780	277.0667			10.2	5%			
	3	6	12.7	200	76.2	20880	274.0157			9.3	5%			
H2V3	1	6	12.9	200	77.4	20330	262.6615	267.6	4.30228701	8	4%	4%	0.0057735	6175.928
	2	6	12.8	200	76.8	20760	270.3125			10	5%			
	3	6	12.9	200	77.4	20890	269.8966			8	4%			
H3V1	1	6	12.5	200	75	20660	275.4667	274.7	0.70553368	12	6%	5%	0.01125833	5133.956
	2	6	12.5	200	75	20580	274.4			12	6%			
	3	6	12.5	200	75	20560	274.1333			8.1	4%			
H3V2	1	6	12.7	200	76.2	20620	270.6037	269.5	2.81584053	9.6	5%	4%	0.0034641	6124.55
	2	6	12.6	200	75.6	20530	271.5608			8.4	4%			
	3	6	12.8	200	76.8	20450	266.276			8.4	4%			
H3V3	1	6	13.3	200	79.8	21050	263.7845	263.1	1.64646603	10.1	5%	4%	0.00606218	6048.641
	2	6	12.8	200	76.8	20300	264.3229			8	4%			
	3	6	12.9	200	77.4	20220	261.2403			8	4%			

Lampiran 5. Data pengujian Impak

Tabel Pengujian Impak

Variasi	α	β	W	l	Cos α	Cos β	WI	COS($\beta-\alpha$)	H0	H1	ΔE	Standar Deviasi	Energi Impak
H1V1	90	70.5	93	0.83	6.12574E-17	0.333806859	77.35185	0.333807	0.83	0.552940307	25.82058	1.096876469	26.45
	90	69	93	0.83	6.12574E-17	0.35836795	77.35185	0.358368	0.83	0.532554602	27.72042		
	90	70.5	93	0.83	6.12574E-17	0.333806859	77.35185	0.333807	0.83	0.552940307	25.82058		
H1V2	90	71	93	0.83	6.12574E-17	0.325568154	77.35185	0.325568	0.83	0.559778432	25.1833	2.581595801	22.61
	90	73	93	0.83	6.12574E-17	0.292371705	77.35185	0.292372	0.83	0.587331485	22.61549		
	90	75	93	0.83	6.12574E-17	0.258819045	77.35185	0.258819	0.83	0.615180193	20.02013		
H1V3	90	75	93	0.83	6.12574E-17	0.258819045	77.35185	0.258819	0.83	0.615180193	20.02013	2.685380226	22.17
	90	71	93	0.83	6.12574E-17	0.325568154	77.35185	0.325568	0.83	0.559778432	25.1833		
	90	74	93	0.83	6.12574E-17	0.275637356	77.35185	0.275637	0.83	0.601220995	21.32106		
H2V1	90	74.5	93	0.83	6.12574E-17	0.267238376	77.35185	0.267238	0.83	0.608192148	20.67138	3.57032611	24.53
	90	71	93	0.83	6.12574E-17	0.325568154	77.35185	0.325568	0.83	0.559778432	25.1833		
	90	69	93	0.83	6.12574E-17	0.35836795	77.35185	0.358368	0.83	0.532554602	27.72042		
H2V2	90	73	93	0.83	6.12574E-17	0.292371705	77.35185	0.292372	0.83	0.587331485	22.61549	0.747341152	22.18
	90	73	93	0.83	6.12574E-17	0.292371705	77.35185	0.292372	0.83	0.587331485	22.61549		
	90	74	93	0.83	6.12574E-17	0.275637356	77.35185	0.275637	0.83	0.601220995	21.32106		
H2V3	90	73.5	93	0.83	6.12574E-17	0.284015345	77.35185	0.284015	0.83	0.594267264	21.96911	0.374153539	21.75
	90	74	93	0.83	6.12574E-17	0.275637356	77.35185	0.275637	0.83	0.601220995	21.32106		
	90	73.5	93	0.83	6.12574E-17	0.284015345	77.35185	0.284015	0.83	0.594267264	21.96911		
H3V1	90	71	93	0.83	6.12574E-17	0.325568154	77.35185	0.325568	0.83	0.559778432	25.1833	2.2298651	23.90
	90	74	93	0.83	6.12574E-17	0.275637356	77.35185	0.275637	0.83	0.601220995	21.32106		
	90	71	93	0.83	6.12574E-17	0.325568154	77.35185	0.325568	0.83	0.559778432	25.1833		
H3V2	90	74	93	0.83	6.12574E-17	0.275637356	77.35185	0.275637	0.83	0.601220995	21.32106	0.751090812	20.89
	90	75	93	0.83	6.12574E-17	0.258819045	77.35185	0.258819	0.83	0.615180193	20.02013		
	90	74	93	0.83	6.12574E-17	0.275637356	77.35185	0.275637	0.83	0.601220995	21.32106		
H3V3	90	75	93	0.83	6.12574E-17	0.258819045	77.35185	0.258819	0.83	0.615180193	20.02013	0.754611682	19.58
	90	75	93	0.83	6.12574E-17	0.258819045	77.35185	0.258819	0.83	0.615180193	20.02013		
	90	76	93	0.83	6.12574E-17	0.241921896	77.35185	0.241922	0.83	0.629204827	18.71311		

Lampiran 6. Data Pengujian Bending

Tabel Hasil Pengujian Bending

FACE BEND								
Variasi	Spesimen	b	d	L	F _m	σ_m	Rata-rata	Standar Deviasi
H1V1	1	38	6	70	4440	340.7895	336.2187	10.42609
	2	38.98	5.9	70	4440	343.5788		
	3	38.2	6.1	70	4390	324.2879		
H1V2	1	38.98	6	70	4480	335.2146	340.2143	7.214468
	2	38.78	6	70	4480	336.9434		
	3	38.5	6	70	4600	348.4848		
H1V3	1	39	6	70	4520	338.0342	340.7316	13.49617
	2	38	6	70	4630	355.3728		
	3	38.5	6	70	4340	328.7879		
H2V1	1	39	6.1	70	4280	309.6769	323.3467	12.12434
	2	39	6	70	4450	332.7991		
	3	39	6	70	4380	327.5641		
H2V2	1	38.4	6	70	4330	328.8845	325.3897	22.15995
	2	38.3	6.28	70	4340	301.69		
	3	38.4	6	70	4550	345.5946		
H2V3	1	38.7	6	70	4010	302.2179	305.5529	5.369461
	2	39.6	6.18	70	4360	302.6939		
	3	38.56	6.1	70	4260	311.7469		
H3V1	1	38.7	6	70	4350	327.8424	326.9837	7.603525
	2	39.5	6	70	4320	318.9873		
	3	39	5.9	70	4320	334.1215		
H3V2	1	38.34	6	70	4160	316.4667	322.683	6.678389
	2	37.7	6	70	4160	321.8391		
	3	38.3	6	70	4330	329.7433		
H3V3	1	38.4	6.2	70	2630	187.0813	215.5452	25.11058
	2	38	6.2	70	3130	224.9918		
	3	38.92	6	70	3130	234.5624		

ROOT BEND								
Variasi	Spesimen	b	d	L	Fm	σ_m	Rata-rata	Standar Deviasi
H1V1	1	38.74	5.9	70	4130	321.5701	317.2543	7.764927
	2	38.7	5.9	70	4130	321.9025		
	3	38.6	6	70	4080	308.2902		
H1V2	1	38.94	5.9	70	3670	284.2859	285.2645	2.668162
	2	38	6	70	3690	283.2237		
	3	38.4	5.9	70	3670	288.2837		
H1V3	1	38.4	6	70	3270	248.3724	246.6665	1.607495
	2	38.9	6	70	3270	245.1799		
	3	38.7	6	70	3270	246.447		
H2V1	1	39	6.4	70	4320	283.9543	298.8435	19.55059
	2	38.8	6	70	4270	320.9837		
	3	38.74	6.3	70	4270	291.5926		
H2V2	1	38.4	6	70	3700	281.033	289.4481	22.41558
	2	39.3	6.2	70	3920	272.4579		
	3	38.8	5.9	70	4050	314.8535		
H2V3	1	38.4	6.22	70	3270	231.1134	229.6774	5.30318
	2	38.9	6.28	70	3270	223.8042		
	3	38.4	6.18	70	3270	234.1148		
H3V1	1	37	6	70	1960	154.5045	149.2986	4.534913
	2	38.84	6	70	1960	147.185		
	3	39.1	6	70	1960	146.2063		
H3V2	1	39.38	6.12	70	2410	171.5646	173.278	4.087872
	2	38.74	6.22	70	2540	177.9437		
	3	38.9	6.18	70	2410	170.3255		
H3V3	1	38.6	6.2	70	1730	122.4235	131.6894	8.287328
	2	39.2	6	70	1860	138.3929		
	3	38.84	6.12	70	1860	134.2518		